Effects of accelerating and decelerating tramway loads on bituminous pavement

Ferhat Hammoum, Armelle Chabot, Denis St Laurent, Hugues Cholet, Bogdan Vulturescu

Materials and Structures (2009) 42:35–49 - DOI 10.1617/s11527-008-9365-y

Effects of accelerating and decelerating tramway loads on bituminous pavement

Ferhat Hammoum*, Armelle Chabot*, Denis St-Laurent**, Hugues Chollet***, Bogdan Vulturescu***

**Laboratoire Central des Ponts et Chaussées – Nantes Atlantique Université*
Route de Bouaye – BP 4129 - 44341 Bouguenais Cedex France
Phone: 00(33)2 40 18 57 67, Fax: 00(33)2 40 18 59 94 - E-mail: ferhat.hammoum@lcpc.fr
***Ministère des Transports du Québec - 930 chemin Sainte-Foy, 5th floor*
Québec QC G1S 4X9 Canada
**** Institut National de Recherche sur les Transports et leur Sécurité*
2 rue de la butte verte, F- 93166 Noisy le Grand Cedex – France

Abstract: The concept of a tramway on tires will allow authorities to provide a modern and efficient transportation system that is well suited to medium-sized towns and suburbs of larger urban areas. Precision in terms of levelling and evenness plays a very important role in the proper functioning of vehicles and in user comfort. These requirements can be satisfied through adequate mechanical resistance against rutting, cracking, and fatigue, and through adequate behaviour of the materials within the structure. These facts motivated the authors to conduct a material and structure study pertaining to the effects of speed and the horizontal forces acting on viscoelastic surface layers that could possibly affect the pavement design. In order to study the various effects of moving loads (braking, accelerating and cornering) on bituminous pavement, numerical calculations were carried out with the help of the ViscoRoute Software version 1.0. The study revealed that the surface layer is subjected to the highest degree of longitudinal shear stress at the driving axles when the tramway is braking or accelerating. These effects decrease with the depth of the pavement materials. The first and second stress invariants (mean stress and deviator stress) are used to show the stress path under the accelerating and braking tramway. When the temperature increases, the same description can be applied to the various load conditions. The stress invariants provide valuable insight into the three-dimensional response of the material, and may be useful in terms of introducing a yield surface for modelling permanent deformations and a more realistic experimental protocol for evaluating the behaviour of bituminous surfacing materials in the laboratory.

Keywords *tramway, pavement, semi-analytical modelling, viscoelasticity, tangential forces, stress path*

1. Introduction

Significant investments have been designated for urban public transportation over the last several years. The concept of a tramway on tires provides a modern and efficient transportation system that is well suited to medium-sized towns and suburbs of larger urban areas (Kühn and Soulas, 2001).

In addition, the construction of a public transportation system is often part of a global urban improvement project that generates many different types of work. Beyond the "basic" requirements pertaining to functionality and durability, making urban environments attractive to the eye has become increasingly important.

The cost of operating a tramway on tires can be reduced if the structural capacity of the pavement is adapted in order to take into account the load on the tramway axle and the number of axle passes (Kühn, 1998). In doing so, significant savings can be realized with respect to the infrastructures.

Early in 2002, the Mixed Public Transportation Syndicate (*Syndicat Mixte des Transports en Commun* – SMTC) of the city of Clermont-Ferrand (France) selected a tire-mounted system for its first 14-km long tramway line, which comprised of 31 stations (Fig. 1).

This innovative vehicle is equipped with an integral guidance system that consists of two V-shaped rollers that grip a central rail. Construction began in 2003, and the first 10-km section was commissioned in November 2006.

The tramway uses a purpose-built section of reserved road that is also designed to act as a 'buffer' between the pedestrian area and the public road.

Fig. 1 The tramway on tires (STE4) used in the city of Clermont-Ferrand - France

The tramway is mounted with Michelin 385/65 R22.5 single-radial tires. The vehicle draws energy from overhead electric wires, like a conventional tram, and is guided by a fixed rail installed in the ground. This central guidance rail is grasped by a pair of metal guide wheels that are set at a 45° angle to the surface of the pavement (Fig. 2). The weight of the vehicle is supported by rubber tires mounted on bogies that are attached to the guide wheels.

Fig. 2 Central guidance system mounted on the wheel axle

In terms of the functionality and characteristics of the tramway line, one can observe that the movement of the tramway is very different from the movement of a heavy truck on a motorway.

Each tramway requires a certain amount of service time at the stations, and there is a minimum safe spacing of 6 minutes between tramways in motion. Thanks to the guidance system, each vehicle follows exactly the same track, with no deviation. However, the load imposed by the tires can vary, and may exhibit significant variability due to transverse and longitudinal forces near stations and curved sections.

Vertical dynamic loads are determined by the vertical vehicle motions and by its suspension system. The forces applied during acceleration, deceleration, steering, or ascent of the vehicle determine the vertical and horizontal dynamic loads.

When a uniform, free-rolling wheel motion is applied against a flat pavement, the longitudinal stress corresponds to the resistance of the rolling tire, which is very low. It is even lower for wide-base single-tire assemblies, which have a lower rolling resistance level.

During vehicle acceleration, turning, climbing, braking, or even uniform vehicle motion (overcoming air resistance and rolling resistance), horizontal forces must be transferred by some of the vehicle's tires, giving rise to increased horizontal stresses on the pavement structure. When this driving or braking torque is applied against the tire assemblies, its effect must be taken into account (Hajj et al., 2005; Al-Qadi and Yoo, 2007). In terms of vehicle motion (load duration, acceleration, braking), classic pavement design tools that are based on linear elastic modelling cannot accurately predict the effects of load conditions on the pavement structure. The objective of this paper is to study these effects using more suitable modelling tools.

In the same way, the transverse stress is close to zero when no transverse force is applied. If macroscopic transverse force is applied against the tire assemblies (e.g.: when the vehicle is turning), this influence must also be taken into account.

Precision in terms of levelling and evenness plays an important role in the proper functioning of vehicles, not to mention user comfort. The mechanical properties

of the surface layer must take into account these requirements for maintaining the guidance system in suitable condition.

A pavement design is considered to be safe when the allowable number of standard axle repetitions is greater than the applied number of standard axle repetitions during the design period, taking into account the fatigue life.

In the case of transport on tires, even on dedicated lanes, proper skid resistance of the wearing course is an absolute necessity, because many types of incidents can occur (e.g.: pedestrians, unauthorized vehicles crossing the lane, large objects falling in the travel path). This requirement for the wearing course is also important in terms of environmental conditions, including the effect of freezing during the winter period.

Overall, the surface must provide adequate skid resistance at medium and low speeds (i.e.: rather rough macro-texture, excellent micro-texture, and low rolling noise), which means a small maximum aggregate size and high void content.

These requirements are combined with the need for mechanical resistance to rutting, ravelling (Hamlat et al., 2007), cracking (Hammoum et al., 2009), and fatigue. A compromise can be achieved by using a slightly open bituminous material with a relatively high coarse-particle content and a gap-graded formulation.

These facts motivated the authors to conduct a detailed study pertaining to the effect of longitudinal and transverse forces on bituminous surface layers that could possibly affect the mechanical performance.

Tramway load characteristics are described in Section 2. The measurement of the longitudinal acceleration signal on the front-left traction wheel of the Clermont-Ferrand tramway gives some information concerning the major forces acting on the wheel. Section 3 presents the structure of the pavement comprised of bituminous materials and the properties of the materials. The mechanical study refers to a pavement structure with a thin bituminous surface layer (BBME) and a thick bituminous base layer loaded by a traction wheel under various load conditions (free-rolling, decelerating, or accelerating).

In this paper, we propose a numerical calculation that takes into account the viscoelastic behaviour of bituminous materials and moving loads on pavement in order to study the effect of various load conditions. The software used (ViscoRoute) and its modelling assumptions, which have been developed at both LCPC and ENPC (Duhamel et al., 2005), are summarized in Section 4. Section 5 describes the pavement responses, including stresses, strains, and displacements, at various depths within the structure and under various load conditions (free-rolling, decelerating, or accelerating).

Finally, in order to provide more realistic load conditions for a triaxial laboratory test, the stress paths obtained at a fixed point M in the pavement are described in terms of stress invariants (p = mean stress, q = deviator stress).

2. Characterization of vehicle effects

The Clermont-Ferrand tramway usually travels at a mean speed of approximately 40 km/h. This speed value is used when calculating the pavement response under free-rolling conditions.

In order to ascertain the various components of the load on the wheel axle, acceleration and deceleration have been measured on the tramway of Clermont-Ferrand (Translohr) at various loads. Here, the study focuses on an out-of-service situation, when the tramway is empty.

The longitudinal forces that act at the interface between the tire and the bituminous surface are generated by sliding friction. In other words, braking or accelerating causes longitudinal contact forces between the tire and the surface of the pavement. The resulting force can be high or very low, depending on the location of the axle and the surface characteristics of the pavement. A much slower velocity of 9 km/h is considered for acceleration when the vehicle leaves the station and for deceleration when it approaches the station.

Figure 3 shows an example of the measurement of acceleration signals on the front-left traction wheel during 100 s between Champratel station and Croix de Neyrat station (DEVIN Project, 2007).

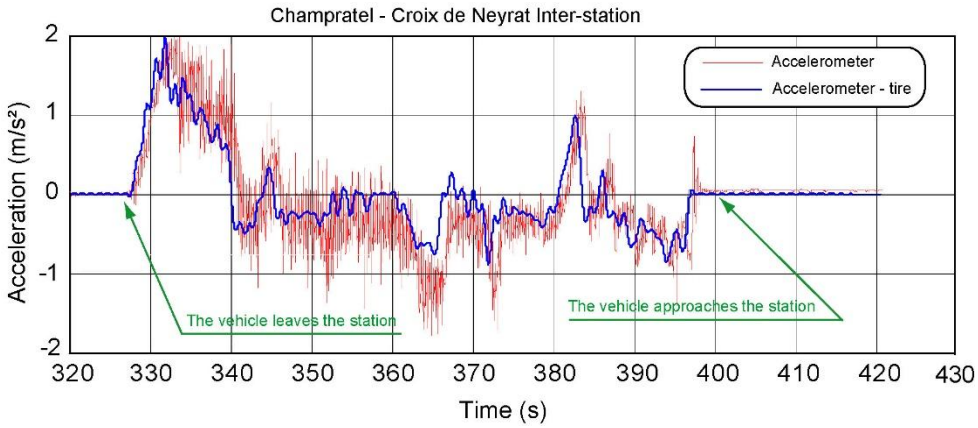

Fig. 3 Accelerations measured on the Clermont-Ferrand tramway (Balay et al., 2007).

After leaving Champratel station, the tramway acceleration climbs to 1.8 m/s² for the first seconds (Fig. 3). After 20 seconds (seconds 340 to 360), the vehicle decelerates at a nearly constant rate of -0.5 m/s² while in a descending slope. The brakes are working harder, resulting in a deceleration peak of approximately -1.5 m/s² just before a 90° curve (seconds 362 to 367). The vehicle then accelerates before the end of the curve (seconds 380 to 387), and finally decelerates in order to stop at Croix de Neyrat station.

A braking effort typically results in a transfer of vertical load from the rear axles to the front axles, and generates shear stresses at the tire-pavement interface. According to the DEVIN Project (2007), a constant deceleration of 1.5 m/s² is used for emergency braking. This deceleration is the rate that is required in order

for a tramway that is travelling at 40 km/h to come to a complete stop at the station.

In order to calculate the corresponding forces between the tires and the pavement surface, the Vocolin program developed by INRETS National Institute has been adapted for the tramway on tires (Fig. 4). With respect to the calculation, the Vocolin program performs three successive steps for each time step of the dynamic problem:

- A search for all possible contact locations between the vehicle's wheels and the pavement profiles, taking into account the acceleration, the speed, and the position of the vehicle.
- A calculation of normal distances between profiles at these locations, and a calculation of corresponding normal forces and then tangential forces
- In the final step, integration of dynamic equations for the next time step.

Figure 4 shows the vehicle configurations that have been simulated by the Vocolin program for the Clermont-Ferrand tramway on tires (Chollet, 2007).

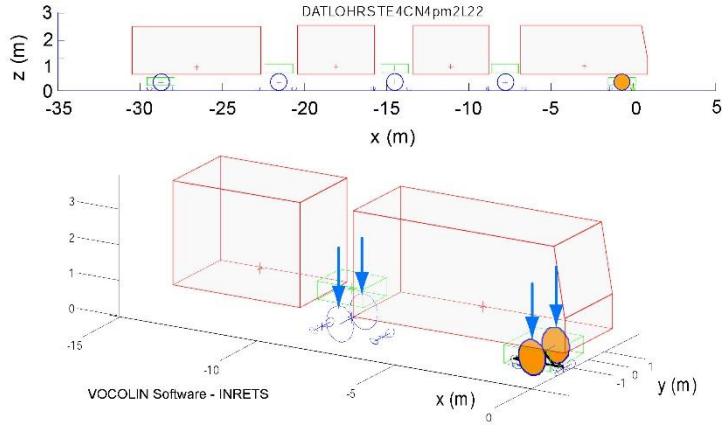

Fig. 4 Vehicle configuration (Chollet, 2007)

The resulting vertical and longitudinal forces on the tires between the Champratel and Neyrat stations are shown in Figure 5. The deceleration from 40 km/h to 0 km/h for the five wheel axles can lead to a “friction” coefficient (horizontal force divided by vertical force).

When the speed is less than 15km/h, the braking effort is distributed among the axles of the tramway. This effort is entirely taken up by the traction axles used for regenerative electric braking. Vehicle simulations based on the above measurements have been conducted in the DEVIN Project (2007). Vehicle configuration and site geometry have been also taken into account. The results are shown in Figure 5, as a function of vehicle position (Chollet, 2007).

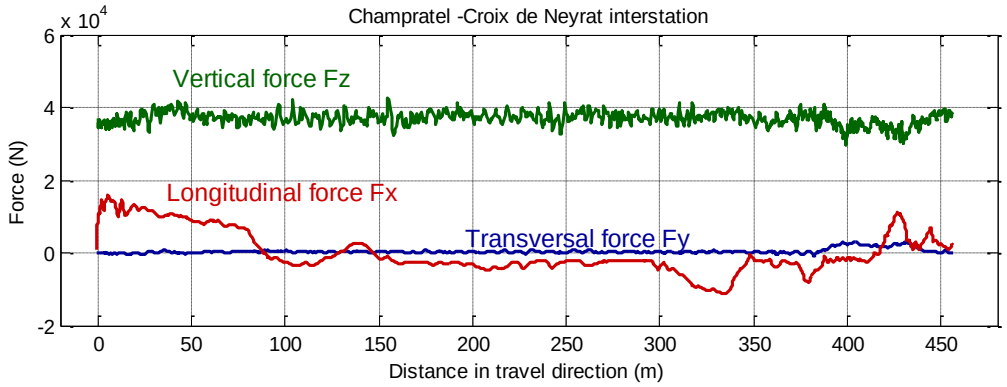

Fig. 5 Calculated forces on the front-left traction wheel (Chollet, 2007)

According to Figure 5, the transverse force F_y that occurs within the 90° turning section demonstrates very low amplitude, and is not considered in the pavement analysis. The braking and accelerating situations are differentiated by the orientation of the longitudinal force, which is negative in the case of deceleration. The maximum horizontal traction effort is attained during the first ten meters ($14\,000\,N$ due to acceleration, with a vertical force of $37\,000\,N$) when the tramway is leaving the station, and at PK 330 just before the 90° turning section ($15\,000\,N$ due to braking, with a vertical force of $38\,500\,N$). Based on these measurements, the pavement response under the conditions of tramway braking and accelerating is calculated at 9 km/h in both cases, with a force of $15\,000\,N$ and $38\,500\,N$ in the longitudinal and vertical directions ($F_x / F_z = 0.39$).

Each tire is inflated to $850\,kPa$ after removing the load supported by the guidance system. A tire contact similar to Pacejka's magic formula is used. For analysis of contact stresses, a model (Chollet, 2009) based on Kalker's Fastsim algorithm of the simplified theory of rolling contact (Kalker, 1982) has been used to define the distribution of shear stresses under the tire. The diagram in Figure 6 illustrates the estimated distribution of pressure under the tire belonging to the previously mentioned tramway.

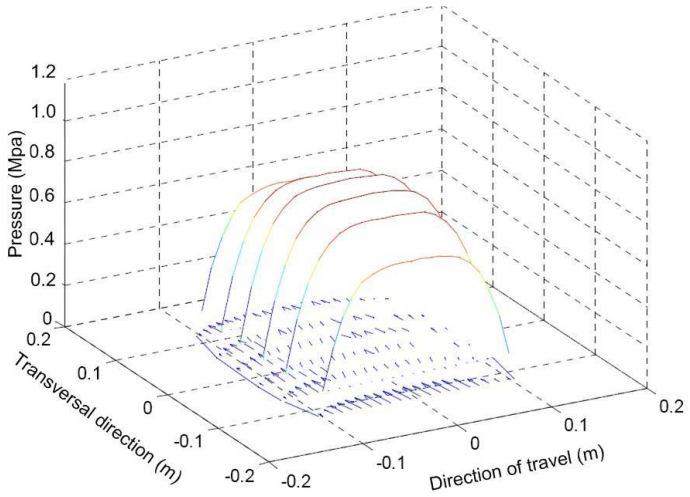

Fig. 6 Calculated distribution of normal pressure under the 385/65 R22.5 tramway tire (DEVIN Project, 2007)

As shown in Figure 6, the contact pressure between the tire and the pavement is distributed quite uniformly over the entire surface, except in the centre.

In this study, the normal contact pressure along the entire area of the tire patch is treated as a constant. Its value is equal to the previously determined vertical force F_z divided by the area of the contact surface of the 385/65 R22.5 tramway tire. The contact area between the tire and the pavement is then assumed to be a rectangle with a width of 0.284 m and a length of 0.226 m in the direction of travel. It should be noted that the contact stress is approximately equivalent to the tire inflation pressure for a ribbed tire. In the case of a continuous rectangular region corresponding to an equivalent smooth tire, the apparent area is estimated as the maximum patch observed at tire contact.
In the first version of the software Viscoroute used here, it is only possible to describe the load as a uniform pressure over a continuous rectangular area. So, the normal contact pressure used in the following simulations according to the results of Figure 6 is then about 0.6 MPa.

3. Pavement structure and material properties

The pavement structure simulated for this tramway study is shown in Figure 7. It is represented as a multi-layered half-space.

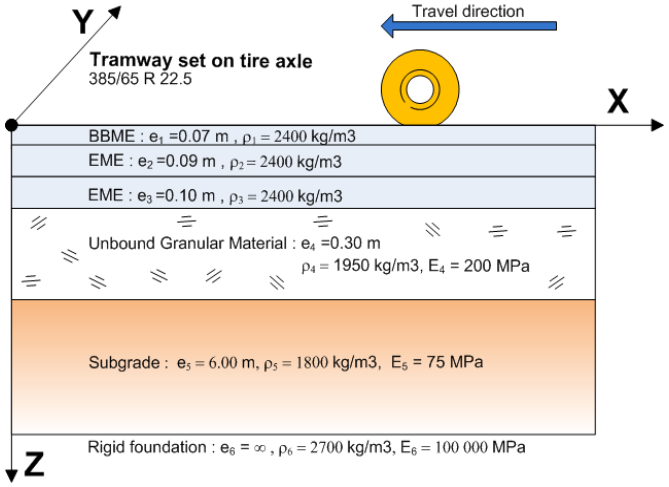

Fig.7 Simulated bituminous pavement structure.

This paper analyzes the pavement structure that is subjected to a traction wheel moving under various load conditions (free-rolling, decelerating, and accelerating).

The longitudinal direction X represents the direction of travel, Y represents the transverse direction, and Z represents the vertical direction measured from the top surface of the pavement. Figure 7 shows a pavement layer system (infinite in the horizontal direction) that is subjected to load from the traction wheel.

The properties of the materials have been fixed from a standard structure similar to the Champratel-Neyrat inter-station site.

Each layer of the structure is considered to be homogeneous and linear, with a constant Poisson's ratio value equal to 0.35. The mechanical behaviour of the soil and the unbound granular material are assumed to be linear and elastic.

The classical BBME bituminous mix (0/10) contains 6.2% bitumen with a 15/25 penetration grade and 4.5% voids. The high modulus EME mix (0/14) contains 5.6% bitumen with a 10/20 penetration grade and 4.1% voids.

Therefore, the material data for the classical bituminous mix (BBME) and the high modulus EME (Table 1) used in the simulation below has been obtained from identical bituminous materials used on site.

The behaviour of the bituminous mixes is modelled using the viscoelastic model proposed initially by Huet (1963, 1999) and Sayegh (1963). The rheological model consists of two parallel branches (Fig. 8). The first one comprises a spring and two parabolic dampers, giving the instantaneous and delayed response of bituminous materials. The second comprises a spring that leads to its static elasticity.

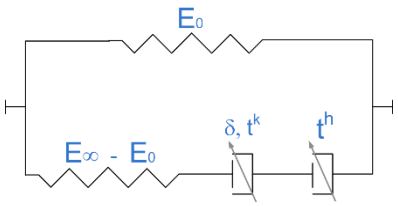

Fig. 8 Principle of the Huet-Sayegh rheological model.

The parameter E_∞ represents the instantaneous elastic modulus, E_0 represents the static elastic modulus, k and h represent the exponents of the parabolic dampers (1>h>k>0), and δ represents a positive dimensionless coefficient that balances the contribution of the first damper to the global behaviour. At frequency ω (where e^{jwt} represents the time variation) and temperature θ, the viscoelastic behaviour is expressed by the following complex modulus:

$$E^*(\omega,\theta) = E_0 + \frac{E_\infty - E_0}{1 + \delta(j\omega\tau(\theta))^{-k} + (j\omega\tau(\theta))^{-h}} \quad (1)$$

where $\tau(\theta) = \exp\left(A_0 + A_1\theta + A_2\theta^2\right)$, which is a function of the temperature depending on three scalar parameters: A_0, A_1 and A_2.

Complex modulus tests have been performed on the two bituminous materials according to French standards. The laboratory results, translated in terms of master curves for both mixes, are illustrated in Figure 9 below.

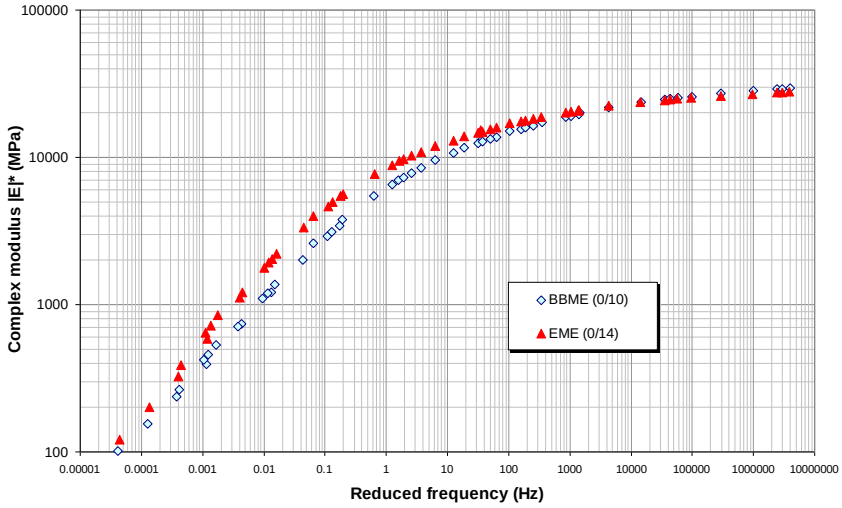

Fig. 9 Master curve data for the two bituminous materials (complex modulus versus reduced frequency)

The Viscoanalyse software (Chailleux et al., 2006) was used to fit the laboratory data and back-calculate the parameters of the Huet-Sayegh model. These values are shown in Table 1.

Table 1 Huet-Sayegh parameters for bituminous materials

Material	E_0 (MPa)	E_∞ (MPa)	δ	k	h	A_0 (t)	A_1 ($t.°C^{-1}$)	A_2 ($t.°C^{-2}$)
BBME	23	34296	2.15	0.18	0.54	4.2036	-0.3883	0.00165
EME	20	31035	2.05	0.19	0.60	5.8384	-0.3877	0.00167

In the following model, the temperature is assumed to be uniform and constant throughout the pavement structure. A temperature of $20°C$ has been chosen as a reference temperature of these calculations.

4. Principles of the ViscoRoute model

Each layer of the pavement is subjected to a complex bending and compression state caused by the effect of the moving load. The amplitudes of the resilient strains remain low, with a magnitude level between 10^{-5} m/m and 10^{-4} m/m. This range can be used to justify why a linear multi-layer model can be considered when carrying out the calculation of strains and stresses, as in the French pavement design guide (SETRA-LCPC, 1997). However, it is important to point out that bituminous mixes exhibit rate- and temperature-dependent behaviour. The assumption of elastic behaviour corresponds to a rough approximation only.

In order to simulate the effect of the braking and acceleration of moving loads, the use of viscoelastic pavement simulations is proposed. A software called ViscoRoute has been developed, based on the modelling of a multi-layered half-space under moving load and using the Huet-Sayegh viscoelastic behaviour of bituminous materials. In this paper, the first version of ViscoRoute is used, programmed in a C++ and Visual Basic® environment. More details pertaining to the modelling and the various applications are given in (Duhamel *et al.*, 2005)

(Chabot et al., 2006) and (Chabot et al., 2009). This version assumes a perfect bond between layers. The latest version 2.0 of ViscoRoute will be soon available (Chupin et al., 2009a 2009b). The new version also allows for slippage between layers to be taken into consideration. The main advantages of ViscoRoute are the ease of use and the short computation time for a multi-layer structure, as compared with the finite element method (FEM) used in the Cesar-LCPC CVCR program (Heck et al., 1998).

To summarize, the proposed method consists of using the Huet-Sayegh model for bituminous mixes and a double Fourier transform to analytically solve the pavement problem in the frequency domain at a given depth. In that domain, the stress fields are written classically, as in equation (2):

$$\sigma^*(k_1,k_2,Z) = 2\mu_i^*(k_1V)\,\varepsilon^*(k_1,k_2,Z) + \lambda_i^*(k_1V)\,tr\left(\varepsilon^*(k_1,k_2,Z)\right)\mathbf{I} \qquad (2)$$

where ε^* represents the strain tensor and where Lame coefficients $\lambda_i^*(k_1V)$ and $\mu_i^*(k_1V)$ depend on the complex modulus $E_i^*(k_1V)$ of the layer i, ($i \in \{1,n\}$).

The analytical solution of the elastodynamic equations leads to a displacement field $U^*\left(U_1^*, U_2^*, U_3^*\right)$ (3), written as a function of the horizontal wave numbers k_1 and k_2, the depth Z, and six parameters for each layer i $\left(\beta_{1i}^-, \beta_{1i}^+, \beta_{2i}^-, \beta_{2i}^+, \beta_{3i}^-, \beta_{3i}^+\right)$.

$$\begin{aligned}
U_1^* &= k_1\beta_{1i}^- e^{-\kappa_p Z} + \kappa_s\beta_{3i}^- e^{-\kappa_s Z} + k_1\beta_{1i}^+ e^{\kappa_p Z} - \kappa_s\beta_{3i}^+ e^{\kappa_s Z} \\
U_2^* &= k_2\beta_{1i}^- e^{-\kappa_p Z} + \kappa_s\beta_{2i}^- e^{-\kappa_s Z} + k_2\beta_{1i}^+ e^{\kappa_p Z} - \kappa_s\beta_{2i}^+ e^{\kappa_s Z} \\
U_3^* &= j\kappa_p\beta_{1i}^- e^{-\kappa_p Z} + jk_2\beta_{2i}^- e^{-\kappa_s Z} + jk_1\beta_{3i}^- e^{-\kappa_s Z} - j\kappa_p\beta_{1i}^+ e^{\kappa_p Z} \\
&\quad + jk_2\beta_{2i}^+ e^{\kappa_s Z} + jk_1\beta_{3i}^+ e^{\kappa_s Z}
\end{aligned} \qquad (3)$$

where $\kappa_p = \sqrt{(1-\frac{V^2}{c_p^2})k_1^2 + k_2^2}$; $\kappa_s = \sqrt{(1-\frac{V^2}{c_s^2})k_1^2 + k_2^2}$; $c_p = \sqrt{\frac{\lambda^* + 2\mu^*}{\rho}}$; $c_s = \sqrt{\frac{\mu^*}{\rho}}$

c_p and c_s represent the longitudinal and shear wave velocities, and ρ represents the density of the material considered.

Using relations (2) and (3), the stress tensor is also obtained as a function of the six parameters of each layer i $\left(\beta_{1i}^-, \beta_{1i}^+, \beta_{2i}^-, \beta_{2i}^+, \beta_{3i}^-, \beta_{3i}^+\right)$. These 6 parameters are determined from boundary conditions for the whole multi-layered medium. In this article, the continuity relationships for the displacements and stresses are used at each interface between layers *i* and *i+1*. The condition at infinity and the load boundary condition on the free surface allow for calculation of the six final parameters and then the displacements and stress fields in the wave number domain. Finally, a double inverse Fourier transform and a specific integration method around the origin point allow the displacements and stresses to be obtained in the real domain.

5. ViscoRoute analysis of the effects of the tramway load

A single load ($F_z = 38,5kN$) moving on the pavement structure described in Figure 7 is studied below, including free-rolling ($V = 40\,km/h, F_x = 0$), accelerating ($V = 9\,km/h, F_x = 15kN$), and decelerating ($V = 9\,km/h, F_x = -15kN$) conditions (see Table 2). The main computed results of mechanical fields are given for a temperature equal to $20°C$, which is assumed to be uniform throughout the structure.

Table 2 Different cases studied using the ViscoRoute model

Case number	Load conditions	Velocity (km/h)	Vertical force (N)	Longitudinal force (N)
C1	Free-rolling	40	38 500	0
C2	Free-rolling	9	38 500	0
C3	Accelerating	9	38 500	+ 15 000
C4	Decelerating	9	38 500	- 15 000

To illustrate the effect of load conditions, all of the results below are shown in the plane y =0.

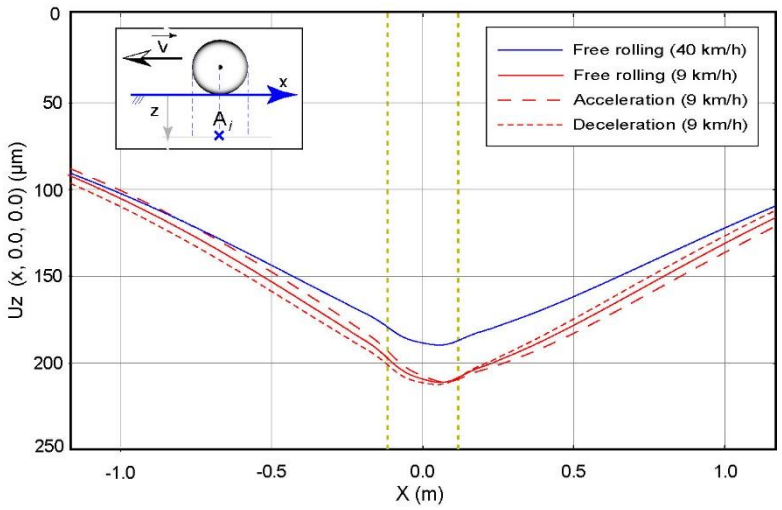

Fig. 10 Pavement deflection for various load conditions (θ=20°C)

In order to identify the effect of velocity on pavement deflection, a calculation was carried out with no horizontal force (i.e.: F_x = 0 N) (Case C2). Figure 10 illustrates the vertical displacement for the various load conditions. As expected, the small values of the speed increase the overall viscoelastic response of the pavement under the wheel, which is not symmetric and which returns to its initial position with a slight delay. In other words, vertical displacement decreases as the velocity of the moving load increases.

In Figure 10, the ratio of forces is equal to 0.39 (see Table 2 for Cases C3 and C4), and the longitudinal force is added for accelerating and decelerating effect. These two load conditions introduce a slight difference in the vertical

displacement. In short, the vertical deflection of the pavement is influenced more by the velocity of the moving load than by the longitudinal forces.

In Figure 11, it can be observed that the shear stress σ_{xz} near the surface of the pavement ($z = 0.0175$ m) is significantly affected by the vehicle motion phases. In contrast to the free-rolling cases, where the shear stress is localized under the load edges regardless of the speed, the accelerating and decelerating load conditions show non-negligible shear stress components under the entire load surface (Fig. 11a). The tension stress component σ_{xx} exists in the various cases studied here, but increases slightly under the wheel under accelerating and decelerating load conditions, especially in the case of deceleration (Fig. 11b).

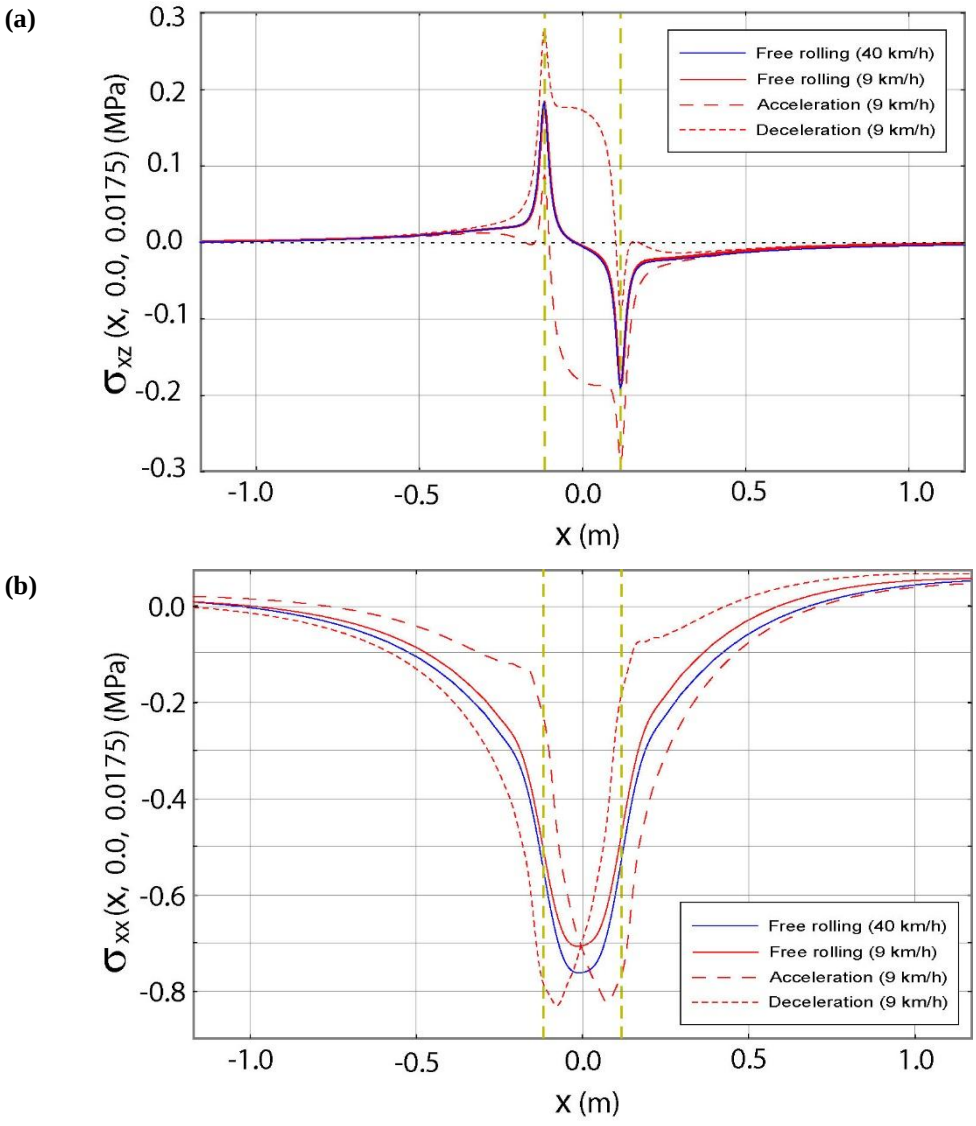

Fig. 11 Components of shear stress (a) and longitudinal stress (b) caused by the tramway under accelerating, braking, and driving conditions

Figure 12 shows the strain fields at the bottom of the bituminous layers (z = 0.2599 m) that are commonly used as criterion in the French design method (SETRA-LCPC, 1997) under free-rolling, accelerating, and decelerating

conditions. In terms of deflection, all components of strain ($\varepsilon_{xx}, \varepsilon_{yy}, \varepsilon_{zz}$) are affected by the low speed, but not in the same order as compared to the effects of accelerating and decelerating load conditions.

(a)

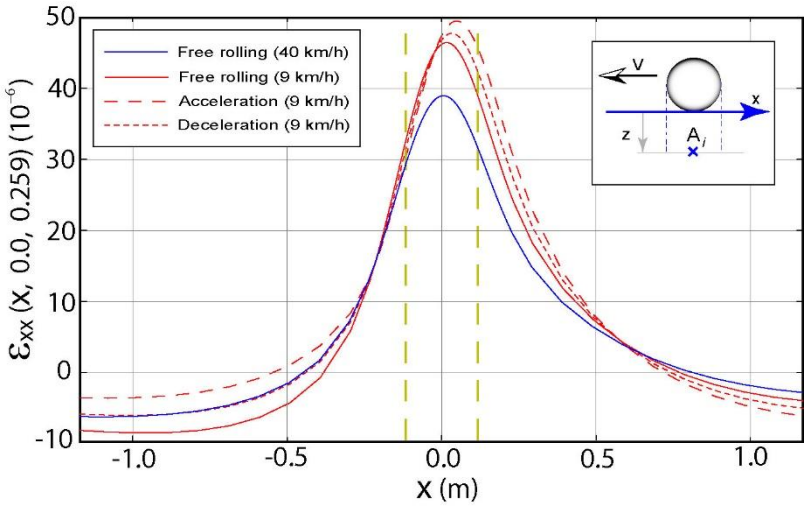

(b)

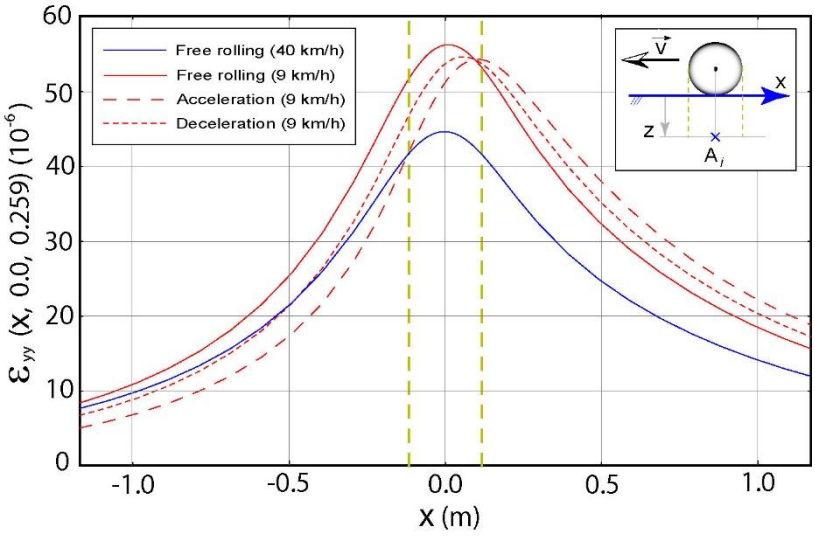

(c)

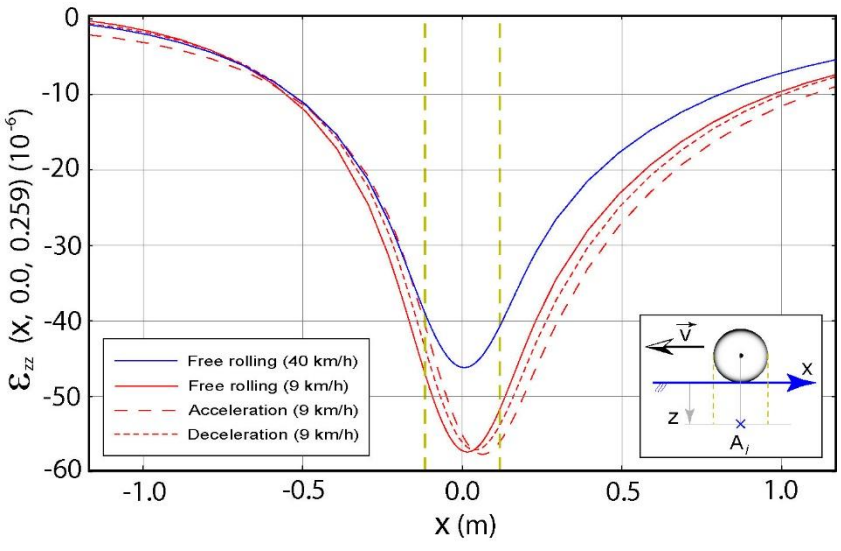

Fig. 12 Strain field ($\varepsilon_{xx}, \varepsilon_{yy}, \varepsilon_{zz}$) (a) , (b) et (c) at the bottom of the bituminous layers under

free-rolling, accelerating, and decelerating load conditions

In conclusion, the braking and accelerating load cases have a significant effect on both stress and the strain field in the region under the tire. Hereafter, we propose an analysis of these results and to design a mechanical test in the laboratory for surfacing materials.

5. Effects of load conditions on the stress path in the pavement

The individual components of a stress tensor are somewhat arbitrary, because the components are identified within the chosen coordinate system. However, the whole tensor is unique, and the full three-dimensional state of stress can be taken into account using invariants. The first and second stress invariants (mean confining stress p and deviator stress q) are classically used in soil mechanics, and are also used as criteria related to plasticity and permanent deformation. These two stress invariants, which are also used in cyclic triaxial laboratory tests on unbound granular materials (Hornych *et al.*, 1998) (Hornych *et al.*, 1999), are defined at a given point M in the pavement by:

$$p(M,t) = -\frac{1}{3}\left(\sigma_{xx} + \sigma_{yy} + \sigma_{zz}\right) \quad \text{(positive in compression)} \tag{4}$$

$$q(M,t) = \frac{1}{\sqrt{2}}\sqrt{\left(\sigma_{xx} - \sigma_{yy}\right)^2 + \left(\sigma_{xx} - \sigma_{zz}\right)^2 + \left(\sigma_{yy} - \sigma_{zz}\right)^2 + 6\left(\sigma_{xy}^2 + \sigma_{xz}^2 + \sigma_{yz}^2\right)} \tag{5}$$

The stress path at point M can be obtained by eliminating the time t between the quantities $p(M,t)$ (Eq. 4) and $q(M,t)$ (Eq. 5). The construction of these paths is proposed in the present case in order to evaluate the effect of the various load conditions.

A yield surface is commonly used to define the transition from elastic behaviour to plastic behaviour in materials that are subjected to static load conditions. The behaviour of the material is elastic while the stress state stays below the yield surface (Fig. 13). When the stress state reaches the yield surface, the surface may evolve in shape and volume. Deformations under these conditions become either permanent or plastic. For isotropic materials, the yield surface can be reduced in its simplest form to a curve in a two-dimensional space defined by stress invariants p and q . This representation is typically used in soil mechanics under static load conditions. The yield surface of a bituminous material that is submitted to cyclic loading is not known. It would probably be much smaller than the yield surface under static load conditions. However, the visualization of stress paths in the (p , q) plane may give qualitative indications. In particular, one can expect an increase of rutting or permanent deformation when the ratio q/p is high. Efforts are currently underway to specify this type of rutting model at LCPC.

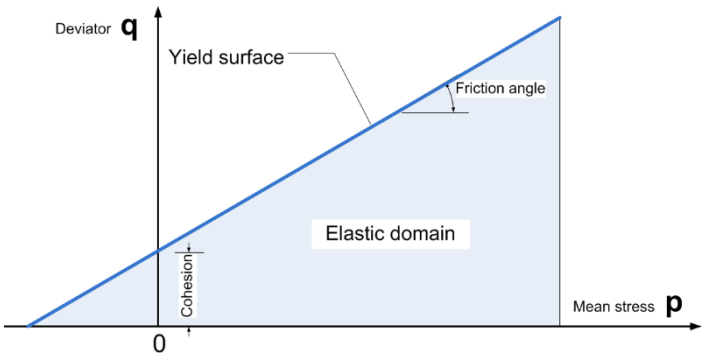

Fig. 13 Typical yield surface in a p-q diagram as used in soil mechanics.

The variations of the stress invariants p and q are plotted in Figures 14 and 15, under the accelerating and braking loads of the tramway. The direction of tire travel is indicated by the arrow. ViscoRoute simulations have been performed for two temperatures (20°C and 40°C). The point α is obtained under the center of the tire (x = 0 m). The point β represents the mechanical state rear under the load edges (x = ± 0.113 m).

In Figure 14, the results shown here are typical of the stress paths obtained near the surface of the pavement. The stress path present in the (p, q) plane has the typical shape of a partially truncated half-sine curve. The maximum value of the deviator q_β is obtained at the point β and the maximum ratio q/p represents two important indicators in the $p-q$ plane. In comparison with the free-rolling load condition, the accelerating and braking load conditions increase the maximum deviator stress q_β by approximately 55 % (20°C) (Fig. 14.a) and approximately 68% (40°C) (Fig. 14.b) at a depth of 0.0175 m. These effects tend to decrease with depth (Fig. 14.c; Fig. 14.d). In other words, the effect of the longitudinal force is observed at the peak value of β. Similarly, the value of α is very different closer to the surface.

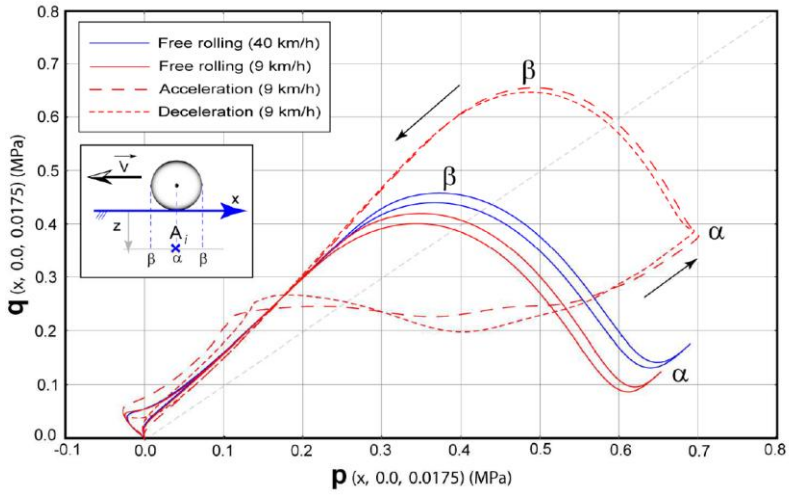

(a) Near the top of the surface layer (**θ = 20°C**)

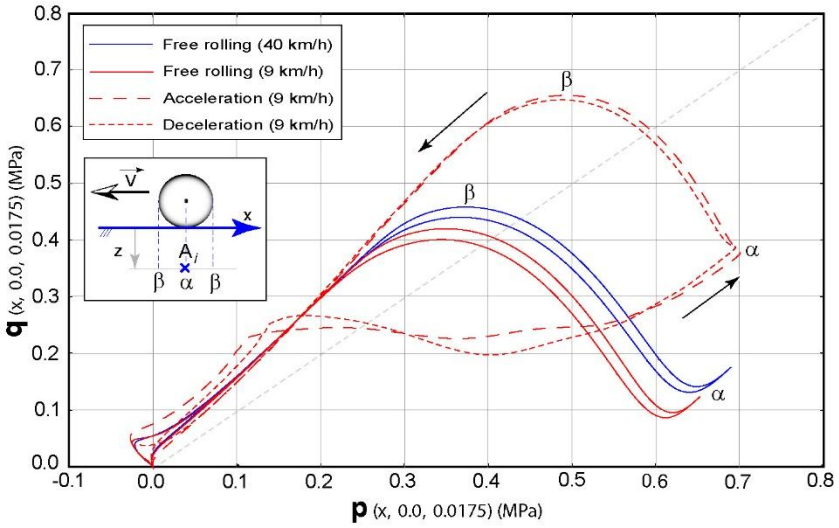

(b) Near the top of the surface layer (**θ = 40°C**)

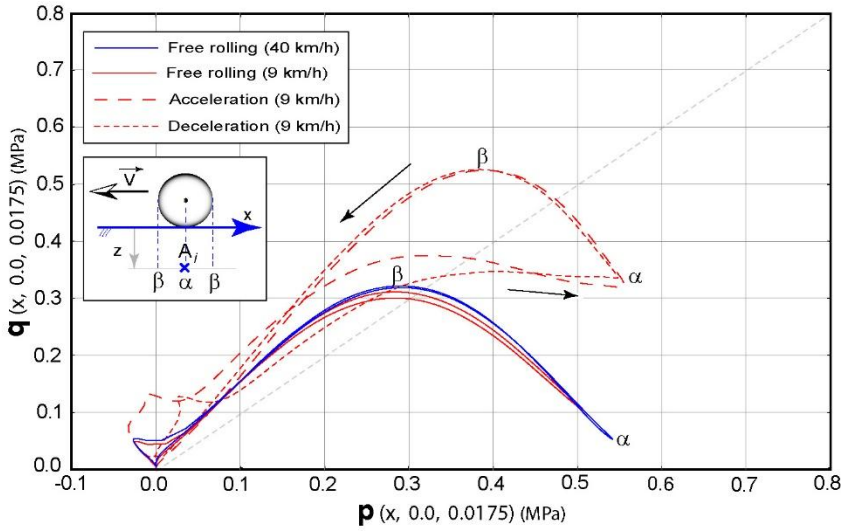

(c) A the bottom of the surface layer **(θ = 20°C)**

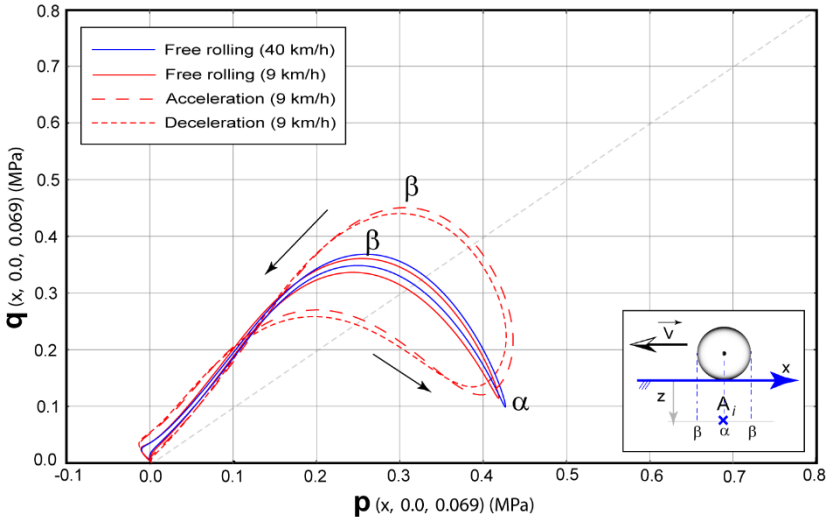

(d) A the bottom of the surface layer (**θ = 40°C**)

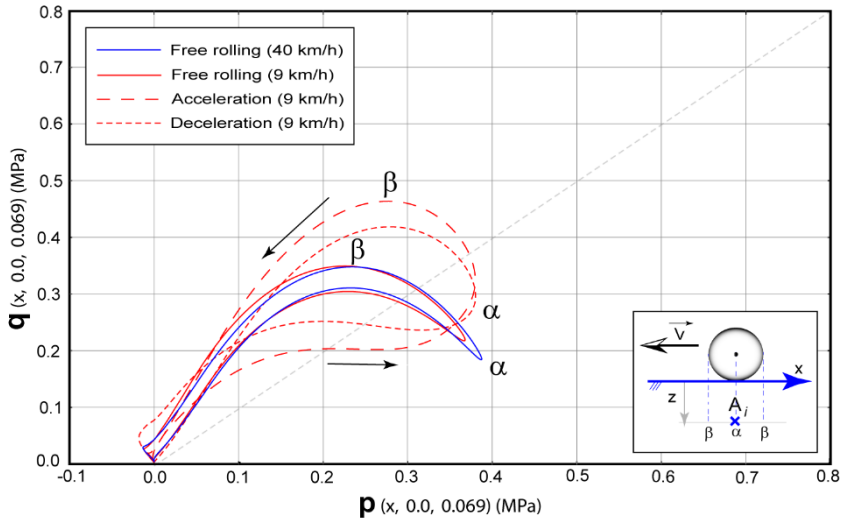

Fig. 14. Stress paths in the surface layer under the free-rolling, braking, and accelerating rolling wheel

In addition, the loading and unloading stresses follow nearly the same path under the free-rolling wheel in the top of the surface layer (Fig. 14b) at 40°C, independently of the speed. Accelerating and decelerating load conditions have a significant effect on the stress path at the bottom of the first bituminous layer (Fig. 14d).

The stress paths have also been computed at the bottom of the base layer (EME) along the direction of the travel axis, as illustrated in Figure 15. Taking into account that the stress intensity in the pavement decreases with the depth, the corresponding location β doesn't represent here a maximum of the stress field. Then, the point β is not represented in the Figure 15.

(a) At the bottom of the base layer (θ = 20°C)

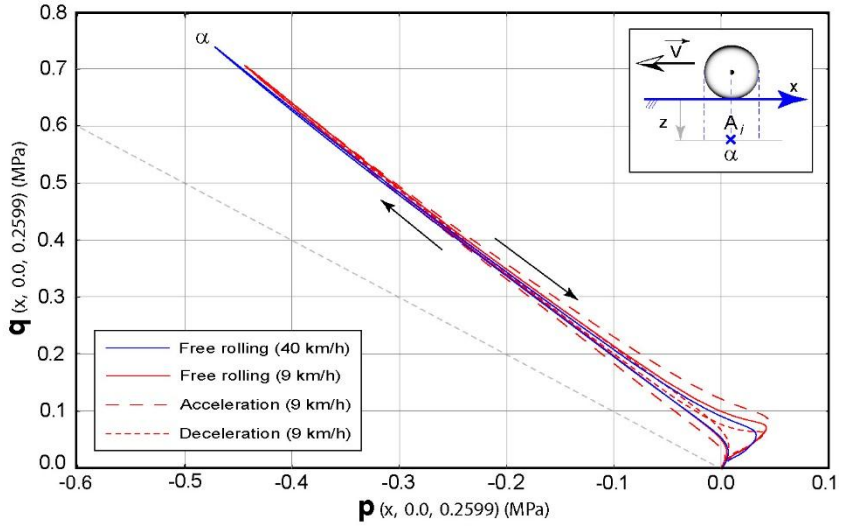

(b) At the bottom of the base layer (θ = 40°C)

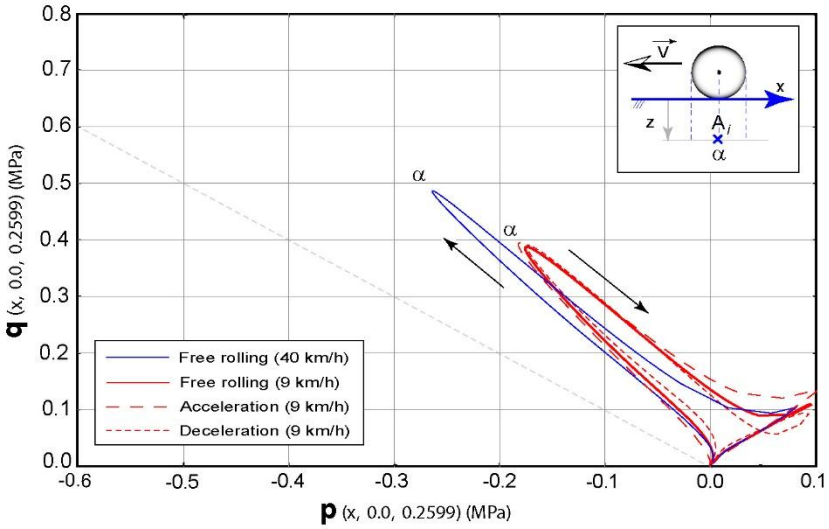

Fig. 15. Stress paths in the second layer under the free-rolling, braking, and accelerating rolling wheel

At the relatively lower temperature (20°C), the loading and unloading conditions follow almost exactly the same path. On the contrary to the surface of the pavement, for this depth, the maximum value of the deviator q_α is located at the point α .

The various load conditions do not affect the stress path at the bottom of the base layer (Fig. 15a). When the temperature increases (summer period), a similar description can be seen for the stress path under the various load conditions (Fig. 15b), but the amplitude of the stress has a lower value.

In summary, simulations based on the stress path caused by braking and accelerating moving loads and the assumption of viscoelasticity lead us to expect significantly more deterioration in the top of the bituminous surface layer due to high shear stresses. This agrees with on-site observations (DEVIN Project, 2007).

6. Conclusions and perspectives

The objective of this paper was to study the effect of the horizontal forces of the moving load of a braking or accelerating tramway on the resilient response of a thick bituminous pavement with a viscoelastic mechanical behaviour, and to provide a description of the mechanical behaviour of the material. The viscoelastic behaviour of bituminous materials was simulated using the Huet-Sayegh model. The ViscoRoute program was used to simulate the viscoelastic response under moving loads.

The deflection and classical strain components (vertical, longitudinal, and transverse strains at the bottom of the bituminous layers) used in the French pavement design method are not strongly affected by the longitudinal forces, as compared with the shear and the distortion components in the top of the thick pavement.

The stress invariants p and q provide valuable insight into the three-dimensional response of the material, and may be useful in terms of introducing a yield surface for modelling permanent deformations and more realistic loading tests aimed at evaluating the behaviour of bituminous materials in the laboratory. At 20°C, the viscoelastic deviatoric stress (q) near the surface increased by 55% under the accelerating and braking load conditions. This increase rose to 68% at 40°C. In light of this, one can expect that braking and accelerating load conditions will generate significantly more rutting in the surface layer.

The modelling cannot be considered to be complete without a prediction of rut depth as a function of load repetitions. Efforts should be pursued to develop permanent deformations or viscoelastoplastic modelling capabilities, including material characterization procedures. A more realistic representation of the non-uniform pressure distributions under the tires is also required in order to improve the quality of the results. Finally, the simulation used here for the tramway can easily be extended to other transportation systems.

7. Acknowledgments

We would like to acknowledge the financial support of the Strategy and Inter-Modal Policies (SI1) sub-division of the Direction of Surface Transportation at MEEDDAT. This work was carried out under the DEVIN project, with the support of National PREDIT program 126-75-01/2004, and the exchange program organized by the Commission Permanente de Coopération Franco-québécoise. The authors would like to express their appreciation to Jean-Michel Piau, Jean-Maurice Balay, and Pierre Hornych for their support throughout this project.

8. References

Al-Qadi I, Yoo P-J (2007) Effect of surface tangential contact stresses on flexible pavement response. The Journal of the Association of Asphalt Paving Technologists 76: 663-692

Chabot A, Tamagny P, Duhamel D, Poché D (2006) Visco-elastic modeling for asphalt pavements – software ViscoRoute. *Proceedings of the 10th International Conference on Asphalt Pavements* (ISBN 978-2-550-49009-8), August 12-17, Québec, Canada, 2: 5-14

Chabot A, Chupin O, Deloffre L, Duhamel D (2009) Viscoroute 2.0: a tool for the simulation of moving load effects on asphalt pavement. *Int. Journal on Road Materials and Pavement Design* Special Issue on Recent Advances in Numerical Simulation of Pavements (in press)

Chailleux E, Ramond G, Such C, de la Roche C (2006) A Mathematical-based Master-curve Construction Method applied to Complex Modulus of Bituminous Materials. *Int. Journal on Road Materials and Pavement Design* 7 (EATA Special Issue): 75-92

Chollet H (2007) Modélisation dynamique et simulations de la rame TRANSLOHR STE4 : Project PREDIT DEVIN. Report INRETS (in French), September 2007

Chollet, H.(2009) - The magic carpet: a surface model for rubber tire contact based on Kalker's methods and Pacejka's coefficients through the STRIPES model, Vehicle systems Dynamics, (under review)

Chupin O, Chabot A (2009a) Influence of sliding interfaces on the response of a viscoelastic pavement. *MAIREPAV6*, Torino, Italy, 6-10 July 2009

Chupin O., Chabot A., Piau J-M, Duhamel D. (2009b) Influence of sliding interfaces on the response of a visco-elastic multilayered medium under a moving load. International Journal of Solids and Structures (under review)

DEVIN Project - Balay JM, Chollet H, Cuisinier D, Hammoum F, Kuhn F. (2007) Project PREDIT DEVIN Durabilité et interaction Véhicule Infrastructure. INRETS-LCPC-LMT, French report

Duhamel D, Chabot A, Tamagny P, Harfouche L (2005) Viscoroute: Visco-elastic modelling for asphalt pavements. *Bulletin des Laboratoires des Ponts et chaussées* (http://www.lcpc.fr/en/sources/blpc/index.php), (258-259): 89-103

Hajj EY, Sebaaly PE, Siddharthan RV (2005) Response of an Asphalt Pavement Mixture under a Slow Moving Truck. *Proceedings of the R. Lytton Symposium on Mechanics of Flexible Pavements*, Baton Rouge, Louisiana, USA

Hamlat S., Hammoum F., Hicher P.-Y., Stefani C. et Terrier J.-P. (2007) Evaluation de la résistance aux efforts tangentiels des revêtements routiers, Bulletin de Liaison des Laboratoires des Ponts et Chaussées, (267) : 49-60

Hammoum F., Chailleux E., Nguyen H-N, Erhlacher A., Piau J.-M. and Bodin D. (2009) Experimental and numerical analysis of crack initiation and growth in thin film of bitumen, International Journal of Road Materials and Pavement Design, 10 (1): 39-61

Heck JV, Piau JM, Gramsammer JC, Kerzreho JP. Odeon H (1998) Thermo-visco-elastic modelling of pavements behaviour and comparison with experimental data from LCPC test track. *Proceedings of the 5th BCRA*, Trondheim, Norway, 6-8 July 1998

Hornych P., Kazai A., Piau J. M. (1998) Study of the resilient behaviour of unbound granular materials, Proceeding of the 5th Conference on Bearing Capacity of Roads and Airfields, Trondheim, Norway, July 1998

Hornych P., Gérard A. (1999) A pneumatic repeated load triaxial apparatus for unbound granular materials and sub-grade soils, *Proceedings of the Workshop on Advances Testing and Modelling of Unbound Granular Materials*, Lisbonne, Portugal, January 1999, Ed. A. Gomes-Correia, Balkema, Rotterdam

Huet C (1963) Etude par une méthode d'impédance du comportement viscoélastique des matériaux hydrocarbonés. PhD dissertation (in French), Faculté des sciences de Paris, France

Huet C. (1999) Coupled size and boundary-condition effects in viscoelastic heterogeneous and composite bodies. *Mechanics of Materials* (31): 787-829

Kalker, J. J. (1982) A fast algorithm for the simplified theory of rolling contact, Vehicle System Dynamics (11): 1-13.

Kühn F, Soulas C (2001) Between bus and light rail, Emergence of intermediate urban systems, A1- Transport modes. *Proceedings of the 89th World Congress on Transport Research (WCTR)*, Seoul (Korea), 23-26 July 2001

Kühn F (1998) Emergence of intermediate urban transit systems: Technical aspects - Mass transit options. *CODATU VIII – Cooperation for urban mobility in the developing world*, Cape Town (South Africa), September 1998

Sayegh G (1963) Contribution à l'étude des propriétés viscoélastiques des bitumes purs et des bétons bitumineux. Ph.D. dissertation (in French), Faculté des Sciences de Paris

SETRA-LCPC (1997) French Design Manual for Pavement Structures. Collection Guides techniques, Ministère de l'Équipement, des Transports et du Logement, France